Accurate measurement of longitudinal cross-relaxation rates in nuclear magnetic resonance

Philippe Pelupessy[a] and Fabien Ferrage
Département de Chimie, Associé au CNRS, Ecole Normale Supérieure, 24 rue Lhomond, 75231 Paris Cedex 05, France

Geoffrey Bodenhausen
Département de Chimie, Associé au CNRS, Ecole Normale Supérieure, 24 rue Lhomond, 75231 Paris Cedex 05, France and Ecole Polytechnique Fédérale de Lausanne, Laboratoire de Résonance Magnétique Biomoléculaire, Batochime, CH-1015 Lausanne, Switzerland

(Received 22 December 2006; accepted 15 February 2007; published online 5 April 2007)

The accuracy of the determination of longitudinal cross-relaxation rates in NMR can be improved by combining symmetrical reconversion with suitable operator swapping methods that lead to the averaging of differences in autorelaxation rates and eliminate the effects of cross relaxation with the environment. The principles are first discussed for an isolated two-spin system comprising a pair of ^{15}N and $^{1}H^{N}$ nuclei subjected to chemical shift anisotropy and dipole-dipole relaxation, and then extended to include further protons. The gains in accuracy are demonstrated experimentally for the protein ubiquitin. © *2007 American Institute of Physics*. [DOI: 10.1063/1.2715583]

I. INTRODUCTION

Cross-correlated relaxation rates have proven to be useful to obtain detailed information on molecular structure,[1,2] internal dynamics,[3–7] and chemical shift anisotropy (CSA) tensors.[8–10] Usually, only transverse cross-correlation rates are measured, but measurements of longitudinal cross-correlation rates can enhance the accuracy of the determination of anisotropic rotational diffusion tensors of proteins and of chemical exchange rates.[11] Correlated fluctuations of the CSA of a spin S (e.g., ^{15}N) and the dipole-dipole (DD) interaction between two spins S and I (e.g., $^{1}H^{N}$) lead to an interconversion of the operators S_z and $2I_zS_z$. This is known as "cross-correlated cross relaxation." The rate of their interconversion, which will henceforth simply be referred to as "cross-relaxation rate," can be evaluated by detecting the decay of the operator P (say, S_z) and by monitoring the buildup of the other term Q (say, $2I_zS_z$) in two separate experiments.[3] However, since the two operators P and Q usually have different autocorrelated relaxation rates ρ_P and ρ_Q, the cross-relaxation rate δ is difficult to quantify.[12,13] Kroenke *et al.*[11] developed a method to overcome this problem: in the interval T where (cross-)relaxation occurs, two "swapping blocks" **S** [each of which comprises a sequence of pulses and delays in the manner of insensitive nuclei enhanced by polarization transfer (INEPT)] are inserted at $T/4$ and $3T/4$ in order to swap the two operators P and Q, so that their autorelaxation rates are averaged. This method greatly enhances the accuracy of the measurement of longitudinal cross-correlation rates, provided the difference of the autorelaxation rates $\Delta=-(\rho_P-\rho_Q)/2$ is not too large compared to the average rate $\rho_{PQ}=(\rho_P+\rho_Q)/2$. However, the introduction of the two swapping blocks **S** may also introduce new systematic errors. Moreover, errors may arise due to differences in the detection efficiencies of the relevant operators P and Q.[14,15] To overcome these problems, we have recently introduced a scheme called "symmetrical reconversion," which was originally designed for the measurement of *transverse* cross-relaxation rates.[14] Instead of merely measuring the decay of the operator $Q=2S_xI_z$ and its conversion into $P=S_x$, we suggested to detect the rates of the decay of both operators P and Q and the two interconversion rates $P\rightarrow Q$ and $Q\rightarrow P$. We demonstrated that this method was accurate, despite differences in detection efficiencies, and that errors arising from violations of the secular approximation remained tolerable even when the scalar couplings are small compared to the line widths. In this article we show that the application of symmetrical reconversion can also increase the accuracy of the measurement of *longitudinal* cross-relaxation rates.

II. THEORY

Figure 1(a) shows the principle of the symmetrical reconversion method. If one starts with an operator P, this term is partially converted into another operator Q due to cross relaxation in the interval T. In order to quantify the extent of this interconversion, both operators Q and P must be detected in separate experiments. However, it is difficult, if not impossible, to have the same detection efficiency for both operators, since their transformation into observable signals must follow distinct pathways that are prone in different ways to relaxation and nonideal rf pulses. Therefore, we suggested that four complementary experiments be used to record the decays of the operators P (sequence I) and Q (IV) and the conversion of P into Q (II) and of Q into P (III). The ratio of the signal amplitudes defined in Eq. (1) depends neither on the efficiency of the initial excitation of P and Q nor on the efficiency of their detection. In the case of trans-

[a]Tel.: (33) 1 44 32 33 89; Fax: 1 44 32 33 97. Electronic mail: philippe.pelupessy@ens.fr

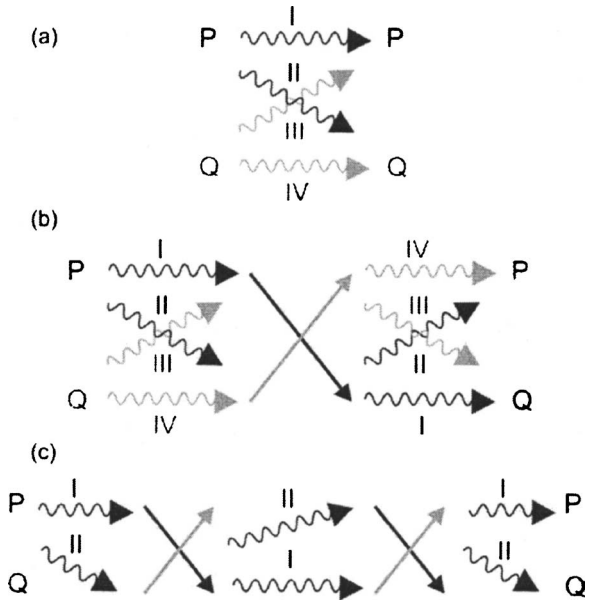

FIG. 1. Principle of the symmetrical reconversion approach. (a) In a system comprising two operators P and Q, one records four separate experiments that correspond to four relaxation pathways. (b) To circumvent problems arising from differences Δ in the autorelaxation rates of P and Q and from perturbing cross-relaxation processes to further spins, the two operators P and Q are swapped in the middle of the relaxation delay T. (c) The scheme developed by Kroenke *et al.* where P and Q are swapped twice but only two relaxation pathways are detected.

verse cross-relaxation rates, simulations have shown that the use of symmetrical reconversion also significantly reduces artifacts due to violations of the secular approximation, so that the amplitudes of the four signals A_i recorded with the experiments i=I, II, III, and IV of Fig. 1 obey the following equation to a very good approximation:[14]

$$\sqrt{\frac{A_{\mathrm{II}}(T)A_{\mathrm{III}}(T)}{A_{\mathrm{I}}(T)A_{\mathrm{IV}}(T)}} = \tanh|\delta T|, \tag{1}$$

where δ is the cross-relaxation rate between the operators P and Q.

For measurements of longitudinal cross relaxation, the situation is more complicated. In this work, we first give an analytical treatment of an isolated two-spin system. The averaging of longitudinal autorelaxation rates by symmetrical reconversion is then discussed using an average Liouvillian approach. We also evaluate the effect of competing cross-relaxation pathways, such as proton-proton nuclear Overhauser effects (NOE), in systems with three or more spins, and we show that the deleterious effects of imperfect swapping of the operators P and Q during the relaxation delay can be significantly reduced by symmetrical reconversion and phase cycling. Finally, we investigate the effect of the so-called thermal correction on observables in relaxation measurements.

A. Analytical treatment of a two-spin 1/2 system

The evolution of the spin systems under study will be described in the frame of the homogeneous master equation (HME)[16]

$$\frac{d\sigma(t)}{dt} = -\hat{L}(t)\sigma(t), \tag{2}$$

where $\hat{L}(t)$ is the Liouvillian superoperator. In all but Sec. II E, where thermal correction factors must be incorporated, the Liouvillian operator will be represented by an effective relaxation matrix. We first consider an isolated two-spin system consisting of $S={}^{15}N$ and $I={}^{1}H^{N}$. The interference between the CSA of the proton and the $N-H^N$ dipole-dipole interaction will be neglected, so that a set consisting of only two operators $P=N_z$ and $Q=2N_zH_z^N$ suffices to describe the evolution of the longitudinal polarization,

$$\frac{d}{dt}\begin{Bmatrix}\langle P\rangle(t)\\ \langle Q\rangle(t)\end{Bmatrix} = -\begin{pmatrix}\rho_P & \delta\\ \delta & \rho_Q\end{pmatrix}\begin{Bmatrix}\langle P\rangle(t)\\ \langle Q\rangle(t)\end{Bmatrix}, \tag{3}$$

where ρ_P and ρ_Q are the autorelaxation rates of the operators P and Q and δ their cross-relaxation rate. This description is quite general and can also be used, *inter alia*, for cross relaxation between $P=C_z'$ and $Q=C_z^\alpha$, or between $P=2C_z'N_z$ and $Q=2C_z^\alpha N_z$.[17] The differential equation can be solved analytically,

$$\begin{Bmatrix}\langle P(T)\rangle\\ \langle Q(T)\rangle\end{Bmatrix} = \exp(-\rho_{PQ}T)\begin{pmatrix}\mathrm{ch}+(\Delta/\Sigma)\mathrm{sh} & -(\delta/\Sigma)\mathrm{sh}\\ -(\delta/\Sigma)\mathrm{sh} & \mathrm{ch}-(\Delta/\Sigma)\mathrm{sh}\end{pmatrix} \times \begin{Bmatrix}\langle P(0)\rangle\\ \langle Q(0)\rangle\end{Bmatrix}, \tag{4}$$

where $\mathrm{ch}=\cosh(\Sigma T)$, $\mathrm{sh}=\sinh(\Sigma T)$, $\rho_{PQ}=(\rho_P+\rho_Q)/2$, $\Delta=-(\rho_P-\rho_Q)/2$, and $\Sigma=\sqrt{\Delta^2+\delta^2}$. The cross-relaxation rate δ_{PQ} can be determined by measuring the decays of P and Q and the interconversion from P to Q and vice versa in four separate experiments, as indicated in Fig. 1(a). For longitudinal relaxation, the ratio of the four signal amplitudes is given by

$$\sqrt{\frac{A_{\mathrm{II}}A_{\mathrm{III}}}{A_{\mathrm{I}}A_{\mathrm{IV}}}} = \sqrt{\frac{\delta^2\mathrm{sh}^2}{\Sigma^2\mathrm{ch}^2-\Delta^2\mathrm{sh}^2}}. \tag{5}$$

Equation (5) reduces to Eq. (1) when Δ is negligible, i.e., when $\rho_Q\approx\rho_P$. Neither of the ratios of Eq. (1) or (5) depends on the efficiency of the initial excitation or detection of the operators P and Q. For short relaxation times T both ratios of Eqs. (1) and (5) can be approximated by $|\delta T|$. For longer delays, the ratio of Eq. (5) is affected by Δ. To obtain an estimate of Δ one can take the dependence on T of the ratio of the signal amplitudes of experiments IV and I,

$$\frac{A_{\mathrm{IV}}}{A_{\mathrm{I}}} = C\frac{\Sigma\mathrm{ch}-\Delta\mathrm{sh}}{\Sigma\mathrm{ch}+\Delta\mathrm{sh}}, \tag{6}$$

where the constant C accounts for the unequal efficiencies of initial excitation and detection of the operators P and Q in the two experiments. The ratio of Eq. (6) can be approximated up to second order in T by $C(1-\Delta T+\Delta^2T^2/2)$. Hence, one can obtain the cross-relaxation rate δ and the difference Δ by fitting simultaneously the experimental intensities of Eqs. (5) and (6).

Symmetrical reconversion is a general concept applicable to any cross-relaxation mechanism. However, when there are competing cross-relaxation mechanisms (such as

proton-proton NOE's in proteins) the approximation of an isolated spin system is not appropriate, particularly if the competing cross-relaxation rates are larger than the one of interest. This problem will be more important if, as in the present study of CSA/DD cross correlation, the protein is not deuterated. To overcome this issue, one can swap the operators P and Q in the middle of the relaxation period T, as in Fig. 1(b). The analytical expressions to describe the evolution of the density operator become a bit more cumbersome. The cross-relaxation rate can be approximated by

$$|\delta| = \frac{1}{T}\,\mathrm{atanh}\left(\sqrt{\frac{A_{\mathrm{II}}A_{\mathrm{III}}}{A_{\mathrm{I}}A_{\mathrm{IV}}}}\right) \Bigg/ \left\{1 + \frac{1}{24}\Delta^2 T^2 + O(T^4)\right\}, \tag{7}$$

where $O(T^4)$ represents other terms that are proportional to T^4 and higher orders. When $\Delta T \ll 1$ this reduces to Eq. (1) and immediately gives the cross-relaxation rate δ. Otherwise, Δ can be obtained from the dependence on T of the ratio of the signal amplitudes of experiments II and III,

$$\frac{A_{\mathrm{III}}}{A_{\mathrm{II}}} = C\exp(-\Delta T) \Bigg/ \left\{1 + \frac{1}{6}\delta^2\Delta T^3 + O(T^5)\right\}. \tag{8}$$

In the next section we shall describe the averaging of autorelaxation in terms of average Liouvillians,[16,18,19] which will be helpful in describing the effects of competing proton-proton NOE's and pulse imperfections.

B. Averaging of autorelaxation rates by symmetrical reconversion

An interesting feature of symmetrical reconversion can be verified both by numerical simulations and experiments:[14] the autorelaxation rates ρ_P and ρ_Q of the operators undergoing cross relaxation are averaged very effectively when calculating the product of signal amplitudes $A_{\mathrm{I}}A_{\mathrm{IV}}$ in the denominator of Eq. (1). This averaging effect may also be obtained by manipulating the density operator in the course of the pulse sequence, for example, by swapping the operators P and Q (e.g., N_z and $2N_zH_z^N$). A general expression for the operator that describes such a swapping operation is

$$\hat{S} = \sum_i (X_i^P X_i^{Q^+} + X_i^Q X_i^{P^+}) + \sum_j Y_j Y_j^+, \tag{9}$$

where $\{X_i^P\}$ and $\{X_i^Q\}$ represent the two sets of Cartesian operator products that contain P and Q, respectively, while the set of operators $\{Y_j\}$ completes the basis of the appropriate Liouville space. If the analysis can be reduced to the two-dimensional Liouville subspace spanned by the operators P and Q as in Eq. (2), the ideal swapping of P and Q can be represented by the simple matrix

$$\hat{S}_2^{\mathrm{id}} = \begin{pmatrix} 0 & 1 \\ 1 & 0 \end{pmatrix}, \tag{10}$$

where the subscript 2 indicates the dimension of the Liouville subspace, a convention that will henceforth be followed for all superoperators.

We focus attention on the denominator $D=(A_{\mathrm{I}}A_{\mathrm{IV}})^{1/2}$ in Eq. (1). When both operators σ and A are represented by vectors in Liouville space, the usual expression for an expectation value $\langle A\rangle = \mathrm{Tr}(A\sigma(t))$ can be replaced by $\langle A\rangle = A^+\sigma(t)$, so that D may be written as

$$D = \sqrt{P^+ \exp(-\hat{L}T)PQ^+ \exp(-\hat{L}T)Q^+}. \tag{11}$$

Introducing the superoperator $\hat{S}$ that describes the swapping block **S**, so that $\hat{L}' = \hat{S}^{-1}\hat{L}\hat{S}$, one obtains

$$D = \sqrt{P^+ \exp(-\hat{L}T)\hat{P}\exp(-\hat{L}'T)P}, \tag{12}$$

where $\hat{P}$ is the projection superoperator $\hat{P} = PP^+$. We may perform a Taylor expansion of D. Note that the projector $\hat{P}$ may be introduced on the left or right of any expression between a vector and its transposed form. We may define an average Liouvillian operator

$$\hat{L}_{\mathrm{av}} = \hat{L}^{(0)} + \hat{L}^{(1)} + \hat{L}^{(2)} + \ldots, \tag{13}$$

with

$$\hat{L}^{(0)} = \frac{1}{2}(\hat{L} + \hat{L}'), \tag{14}$$

and

$$\hat{L}^{(1)} = \frac{T}{8}[(\hat{L} - \hat{L}')\hat{P}, (\hat{L} - \hat{L}')], \tag{15}$$

so that one may write

$$D = P^+ \exp(-\hat{L}_{\mathrm{av}}T)P. \tag{16}$$

As long as the auto- and cross relaxation of the operators P and Q is confined to a two-dimensional subspace ($\hat{S} = \hat{S}_2^{\mathrm{id}}$) and described by a symmetrical relaxation superoperator ($\hat{L}' = \hat{L}$), both terms in the commutator of Eq. (15) are diagonal, so that the first-order correction $\hat{L}^{(1)}$ to the average Liouvillian of Eq. (13) vanishes. Exact calculations show that even the second-order correction $\hat{L}^{(2)}$ vanishes in this favorable case. However, if cross relaxation involving a third operator R occurs, and if the cross-relaxation rates σ_{PR} and σ_{QR} are different, the first-order correction $\hat{L}^{(1)}$ does not vanish.

We now examine the numerator in Eq. (1). If the relaxation superoperator is Hermitian, A_{II} and A_{III} are equal. Indeed, we may write

$$\begin{aligned} A_{\mathrm{II}} &= P^+ \exp(-\hat{L}T)Q, \\ A_{\mathrm{III}} &= Q^+ \exp(-\hat{L}T)P. \end{aligned} \tag{17}$$

These amplitudes are both real numbers so that one can write

$$A_{\mathrm{III}} = A_{\mathrm{III}}^T = P^+[\exp(-\hat{L}T)]^T Q = P^+[\exp(-\hat{L}T)]Q = A_{\mathrm{II}}. \tag{18}$$

If the effective relaxation superoperator is *not* Hermitian, for instance because of imperfect swapping of the operators P and Q during the relaxation delay T (*vide infra*), the term that depends to first order on T in the expansion of the numerator $(A_{\mathrm{II}}A_{\mathrm{III}})^{1/2}$ in Eq. (1) is given by the geometric average of the off-diagonal terms in the effective Liouvillian,

$$(A_{II}A_{III})^{1/2} = (L_{PQ}L_{QP})^{1/2}T + O(T^2). \tag{19}$$

C. Effects of proton-proton cross relaxation (homonuclear NOE's)

Consider a system with $N>2$ spins with dipolar cross relaxation between the proton H^N belonging to the pair (I=N, S=H^N) and one or more neighboring protons H. In our study of a nondeuterated protein, we shall consider that H=H^α since this is often the closest proton. In this case, the first-order correction of Eq. (15) does not vanish. For the CSA/DD cross correlation under discussion, the HME can be cast in the following form:

$$\frac{d}{dt}\begin{pmatrix}\langle P\rangle(t)\\ \langle Q\rangle(t)\\ \langle V\rangle(t)\\ \langle W\rangle(t)\end{pmatrix} = -\hat{L}_4\begin{pmatrix}\langle N_z\rangle(t)\\ \langle 2N_zH_z^N\rangle(t)\\ \langle 2N_zH_z^\alpha\rangle(t)\\ \langle 4N_zH_z^NH_z^\alpha\rangle(t)\end{pmatrix} = -\hat{L}_4\begin{pmatrix}\langle P\rangle(t)\\ \langle Q\rangle(t)\\ \langle V\rangle(t)\\ \langle W\rangle(t)\end{pmatrix}, \tag{20}$$

where

$$\hat{L}_4 = \begin{pmatrix}\rho_P & \delta & 0 & 0\\ \delta & \rho_Q & \sigma & 0\\ 0 & \sigma & \rho_V & \delta\\ 0 & 0 & \delta & \rho_W\end{pmatrix}. \tag{21}$$

Note that the cross-relaxation rate δ that connects P and Q is the same as the off-diagonal term δ between operators V and W. The subscript 4 on $\hat{L}_4$ refers to the dimension of the Liouville subspace while $\sigma=\sigma(H^NH^\alpha)$, i.e., the dipolar cross-relaxation (Overhauser) rate between the two nearby protons H^N and H^α. The dipolar coupling between N and H^α has been neglected.

The (ideal) swapping of the longitudinal operators P and Q can be represented by the unitary transformation,

$$\hat{S}_4^{\mathrm{id}} = \begin{pmatrix}0 & 1 & 0 & 0\\ 1 & 0 & 0 & 0\\ 0 & 0 & 0 & 1\\ 0 & 0 & 1 & 0\end{pmatrix}. \tag{22}$$

The first-order average Liouvillian resulting from Eq. (15) corresponding to the symmetrical reconversion scheme of Fig. 1(a) is

$$\hat{L}_{\mathrm{sr}}^{(1)} = \frac{T}{8}\begin{pmatrix}-\sigma^2 & 0 & 0 & 2\Delta\sigma\\ 0 & 0 & 0 & 0\\ 0 & 0 & 0 & 0\\ 2\Delta\sigma & 0 & 0 & \sigma^2\end{pmatrix}, \tag{23}$$

where the subscript sr stands for symmetrical reconversion. From Eq. (23), it is clear that symmetrical reconversion alone is not sufficient to suppress effects of cross relaxation to neighboring protons. Note that all terms would vanish if σ were zero, which would effectively correspond to a system with two isolated spins S=N and I=H^N. Several methods have been developed to suppress proton dipolar cross-relaxation pathways.[20–23] It is possible to symmetrize the cross-relaxation pathways with respect to the autorelaxation rates of the N_z and $2N_zH_z^N$ operators by using the $\hat{S}_4^{\mathrm{id}}$ transformation of Eq. (22) in the middle of the relaxation delay T,[11,24] as in Fig. 1(b). Using this scheme, the zeroth-order average Liouvillian is

$$\hat{L}_4^{(0)} = \begin{pmatrix}\rho_{PQ} & \delta & 0 & \sigma/2\\ \delta & \rho_{PQ} & \sigma/2 & 0\\ 0 & \sigma/2 & \rho_{VW} & \delta\\ \sigma/2 & 0 & \delta & \rho_{VW}\end{pmatrix}, \tag{24}$$

with $\rho_{VW}=(\rho_V+\rho_W)/2$, in analogy to $\rho_{PQ}=(\rho_P+\rho_Q)/2$. If, in addition to swapping the operators in the middle of the interval T as expressed by Eq. (22), one considers the ratio of Eq. (1) in the context of symmetrical reconversion, the first-order correction due to $\hat{L}_4^{(0)}$ vanishes since $\hat{S}_4^{\mathrm{id}-1}\hat{L}_4^{(0)}\hat{S}_4^{\mathrm{id}}=\hat{L}_4^{(0)}$. When using the ratio of Eq. (1) appropriate for symmetrical reconversion, the lowest-order correction to the average Liouvillian, which comes from the zeroth- and first-order Liouvillians $\hat{L}_4^{(0)}$ and $\hat{L}_4^{(1)}$, depends on T^2. It is also possible to cancel the first-order terms by using two swapping transformations $\hat{S}_4^{\mathrm{id}}$ at $T/4$ and $3T/4$ during the relaxation delay as in Fig. 1(c).[11,19] Proton-proton cross-relaxation (Overhauser) effects do not lead to any artifacts, provided two conditions are fulfilled: (i) the Liouvillian superoperator that governs relaxation processes must be invariable to the permutation $\hat{S}_4^{\mathrm{id}}$ of the two cross-relaxing operators P and Q [see Eq. (24)] and (ii) the Liouville subspaces containing the cross-relaxing operators should only be linked by the cross-relaxation rate that one wishes to measure (see Appendix).

D. Effects of imperfect operator swapping transformations

A prerequisite for the use of average Liouvillian theory for the design of relaxation experiments is that transformations intended to swap pairs of operators should be ideal, i.e., that relaxation during the swapping blocks and rf pulse errors can be neglected, so that they can be represented by unitary transformations. If relaxation or any other imperfection affects all operators identically during the swap sequence, the swap operator can be represented by a unitary matrix multiplied by a scalar attenuation factor, for instance $a=\exp(-R_2 2\tau)$ for transverse relaxation, so that average Liouvillian theory is valid.[19] If the nonideality leads to a nonuniform attenuation of different terms in the density operator, the consequences can be more severe. In the pulse scheme of Fig. 2 designed to swap longitudinal one- and two-spin orders N_z and $2N_zH_z^N$, the π pulse applied to the protons at the beginning of the swapping block can be a source of nonideality. Indeed, an improper calibration of this pulse and its unavoidable rf field inhomogeneity lead to deviations from an ideal nutation angle π which affects the two-spin order $2N_zH_z^N$. We can describe these effects in the two-dimensional

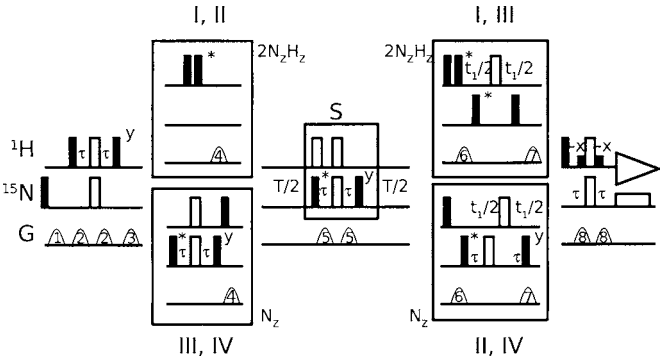

FIG. 2. Pulse sequences for the measurement of the longitudinal cross-correlated cross-relaxation rate δ. Narrow filled and unfilled bars indicate $\pi/2$ and π pulses, respectively, while the wide unfilled rectangle stands for a decoupling sequence and low filled squares for selective $\pi/2$ pulses applied to the water resonance. All pulses are along the x axis unless otherwise indicated. The four pulses marked by an asterisk are phase alternated independently, while changing the receiver sign. The delay $\tau=1/(4J_{\mathrm{NH}})$ is 2.65 ms. A total of four interleaved experiments are performed, each experiment following a different path as indicated in the boxes (see Fig. 1). The central box **S** represents the sequence designed to swap the operators P and Q.

Liouville subspace spanned by operators P and Q by a nonideal asymmetric swapping superoperator $\hat{S}_2^{\mathrm{nid}}$,

$$\hat{S}_2^{\mathrm{nid}} = \begin{pmatrix} 0 & 1-\lambda \\ 1 & 0 \end{pmatrix}, \tag{25}$$

where $0<\lambda\ll 1$ describes the deviation from the ideal swapping transformation $\hat{S}_2$ of Eq. (10). Note that the nonideal π pulses in the middle of the swap sequence lead to a uniform attenuation that does not affect the measured rate. Using an analytical treatment for the scheme of Kroenke *et al.*,[11] the ratio $(A_{\mathrm{II}}/A_{\mathrm{IV}})$ turns out to be

$$A_{\mathrm{II}}/A_{\mathrm{IV}} = -\delta(1-\lambda/2)T + O(T^2) \tag{26}$$

if the operators P and Q are swapped once in the middle of the relaxation delay. If these terms are swapped twice at $T/4$ and $3T/4$, the ratio is

$$\begin{aligned} A_{\mathrm{II}}/A_{\mathrm{IV}} &= -\delta(1-\lambda/2)/(1-\lambda) \\ &= -\delta(1+\lambda/2+O(\lambda^2))T + O(T^2). \end{aligned} \tag{27}$$

On the other hand, the effect of the geometric averages in the denominators $(A_{\mathrm{II}}A_{\mathrm{IV}})^{1/2}$ of Eqs. (1) and (5) used for symmetrical reconversion can be represented by an *ideal* swapping superoperator $\hat{S}_2$. If, in addition to symmetrical reconversion, a single swapping operation represented by $\hat{S}_2^{\mathrm{nid}}$ is applied in the middle of the relaxation period T, the zeroth-order doubly averaged Liouvillian that expresses the evolution of the denominator in Eq. (1) is

$$\hat{L}_{\mathrm{av}}^{(0)} = \begin{pmatrix} \rho_{PQ} & \delta(1-\lambda/2)^2/(1-\lambda) \\ \delta(1-\lambda/2)^2/(1-\lambda) & \rho_{PQ} \end{pmatrix}. \tag{28}$$

The off-diagonal elements can be expanded as $\delta(1-\lambda/2)^2/(1-\lambda)=\delta\{1+\lambda^2/4+O(\lambda^3)\}$. The first-order coefficient in the Taylor expansion of the numerator $(A_{\mathrm{II}}A_{\mathrm{III}})^{1/2}$ of Eqs. (1) and (5) does not show any first-order dependence on λ. Therefore, the systematic error on the measured rate is attenuated below the detection threshold, even for values of λ as large as 0.1 (which corresponds to a nonideal nutation on the proton through 165° instead of 180°).

Another source of artifacts, which is important when measuring small cross-relaxation rates, is the partial conservation of the initial operators in the swapping transformation, i.e., the presence of residual terms along the diagonal of the matrix,

$$\hat{S}_2^{\mathrm{res}} = \begin{pmatrix} \varepsilon & 1 \\ 1 & \varepsilon \end{pmatrix}. \tag{29}$$

For small values of ε, the apparent rate is $\delta-2\varepsilon/T$ with the double swapping method of Kroenke *et al.*[11] and $\delta-\varepsilon/T$ when considering the symmetrical reconversion ratio of Eq. (1). For the shortest delays employed, the relative error on the measured rates may be an order of magnitude larger than ε. In the present study, such a problem would arise if the $\pi/2$ pulses of the block that is supposed to swap P and Q (i.e., N_z and $2N_zH_z^N$) are not ideal (which is inevitable due to imperfect rf homogeneity). This effect was suppressed by phase cycling of the initial $\pi/2$ pulse in the swapping block in Fig. 2.

In conclusion, symmetrical reconversion suppresses the deleterious effects of imperfections of the proton pulses that lead to an asymmetric swap operator [Eqs. (25)–(28)]. rf field inhomogeneities or miscalibration of the nitrogen pulses, which cause residual diagonal terms of the swap operator, are corrected for by phase cycling. Nonideal settings of the fixed delays (due to the dispersion in the values of scalar coupling constants) and relaxation lead to a uniform attenuation of all operators, which only affects the precision and not the accuracy of the measurements.

E. Thermal correction effects

Levitt and Di Bari[18] have shown that it is possible to create several kinds of steady-state terms under multiple-pulse experiments. However, most relaxation measurements of longitudinal polarization or multiple-spin order assume that the spin system evolves towards a saturated or demagnetized steady state where the density operator can be described by a unity operator. In this section, we demonstrate that we do not expect any perturbations from steady-state effects in our experiments.

Using the notation of Ghose,[19] the Liouvillian superoperator $\hat{L}(t)$ of Eq. (2) can be defined as

$$\hat{L}(t) = i\hat{H}(t) + \hat{\Gamma}(t) + \hat{\Theta}(t), \tag{30}$$

where $\hat{H}(t)$ is the Hamiltonian superoperator that contains all coherent terms, $\hat{\Gamma}(t)$ is the relaxation superoperator, and $\hat{\Theta}(t)$ is the thermal correction superoperator. The latter takes into account the evolution of the spin system towards a steady state. In our experiments, the relaxation takes place after a so-called isotope selection which is achieved by alternating the phase of a pulse. This means that the sign of part of the density operator alternates at a given point in a pulse sequence, usually before the beginning of the relaxation period. To take this sign alternation into account, we may ex-

pand the density operator in the basis $\{\boldsymbol{E}/2, Q_i^g, Q_j^u\}$, where $\boldsymbol{E}$ is the identity operator, while the even operators $\{Q_i^g\}$ (g for *gerade*) are invariant and the odd operators $\{Q_j^u\}$ (u for *ungerade*) alternate in sign,

$$\sigma_+(0) = \boldsymbol{E}/2 + \sum_i a_i Q_i^g + \sum_j b_j Q_j^u,$$
$$\sigma_-(0) = \boldsymbol{E}/2 + \sum_i a_i Q_i^g - \sum_j b_j Q_j^u. \tag{31}$$

After a subsequent interval (i.e., a relaxation delay T, a coherent evolution period t_1, etc.) represented by the propagator $\hat{U}$, the density operators are

$$\hat{U}\sigma_+(0) = \hat{U}\boldsymbol{E}/2 + \sum_i a_i \hat{U} Q_i^g + \sum_j b_j \hat{U} Q_j^u,$$
$$\hat{U}\sigma_-(0) = \hat{U}\boldsymbol{E}/2 + \sum_i a_i \hat{U} Q_i^g - \sum_j b_j \hat{U} Q_j^u. \tag{32}$$

Since the signals must be subtracted from each other, the signs of the observable operators are reversed for odd scans (Q_{obs} for even and $-Q_{\mathrm{obs}}$ for odd scans), leading to the net signal,

$$\mathrm{tr}\{Q_{\mathrm{obs}}\hat{U}\sigma_+(0)\} + \mathrm{tr}\{-Q_{\mathrm{obs}}\hat{U}\sigma_-(0)\} = 2\sum_j b_j \,\mathrm{tr}\{Q_{\mathrm{obs}}\hat{U}Q_j^u\}. \tag{33}$$

This corresponds exactly to the signal resulting from two experiments that would both have started with the reduced density operator,

$$\sigma(0) = \sum_j b_j Q_j^u. \tag{34}$$

Thus the isotope filter ensures that the even operators $\{Q_i^g\}$ do not contribute to the observable signal. Moreover, an interesting characteristic of the thermal correction factor can be derived recursively, using the property $\hat{\Theta}^2 = \hat{\Theta}(i\hat{H} + \hat{\Gamma}) = 0$,

$$(i\hat{H} + \hat{\Gamma} + \hat{\Theta})^n = (i\hat{H} + \hat{\Gamma})^n + (i\hat{H} + \hat{\Gamma})^{n-1}\hat{\Theta}, \tag{35}$$

for every natural integer n, so that

$$\exp[-(i\hat{H} + \hat{\Gamma} + \hat{\Theta})t] = \exp[-(i\hat{H} + \hat{\Gamma})t] + \sum_{n=1}^{+\infty} \frac{1}{n!}(i\hat{H} + \hat{\Gamma})^{n-1}\hat{\Theta}. \tag{36}$$

Therefore, $\hat{U}(t)\sigma(0) = \exp[-(i\hat{H} + \hat{\Gamma})t]\sigma(0)$, i.e., the thermal correction is averaged out. Notice, however, that the sign alternation has to be performed *before* the relaxation interval T in the sequence where the thermal correction could affect the evolution of the density operator. If the isotope filter is inserted after the relaxation delay T, the effects of the thermal correction must be taken into account.

III. MATERIALS AND METHODS

All experiments were performed on a Bruker Avance 600 MHz spectrometer with a triple-resonance probe equipped with three orthogonal gradients. A 1.5 mM sample of uniformly ^{15}N labeled human ubiquitin with 50 mM ammonium acetate (pH=4.5) was investigated, except for the temperature dependent experiments, for which a sample of triply labeled [^{2}H, ^{13}C, ^{15}N] ubiquitin with a similar concentration and pH was used.

Figure 2 shows the pulse sequences used for the measurement of the longitudinal cross-relaxation rate δ. After an initial INEPT transfer, the operator $2N_zH_z^N$ is selected in experiments I and II, while this operator is converted into N_z in experiments III and IV. Then a relaxation period T follows. In the center of this period, the operators N_z and $2N_zH_z^N$ are swapped by an INEPT block. The first pulse applied to the ^{15}N nuclei is phase alternated in order to ensure that the diagonal elements of the matrix of Eq. (29) are zero. At the end of the relaxation period T, $2N_zH_z^N$ is detected directly in experiments I and III, while N_z is converted into $2N_zH_z^N$ in experiments II and IV prior to detection. In order to prevent cross contamination between the two desired operators, a proton $\pi/2$ pulse followed by a gradient is used to select N_z, while two $\pi/2$ pulses (the second of which is phase alternated) are applied for the selection of $2N_zH_z^N$. In all experiments the nitrogen-15 coherence evolves in the t_1 interval, giving rise to heteronuclear single quantum correlation (HSQC)-like spectra.

IV. RESULTS

The new approach [Fig. 1(b)] combines the swapping of the operators P and Q (i.e., N_z and $2N_zH_z^N$) in the middle of the relaxation interval T on the one hand and the combination of four signal amplitudes in the manner of symmetrical reconversion. This method was applied to a sample of ^{15}N labeled human ubiquitin. We have also employed the sequence of Kroenke *et al.*[11] [see Fig. 1(c)] with small modifications; instead of including the so-called sensitivity enhanced echo-antiecho sequence[25] we applied the method of States *et al.*[26] for frequency discrimination and Watergate[27] for water suppression. Although, as expected, sensitivity enhancement gives an enhancement of the signal of about 1.4, there are a few disadvantages associated with it. First of all, the net effect of the sensitivity enhancement sequence on the protons which are not coupled to nitrogen-15 is in principle a 2π rotation. Often, this is an advantage since the water magnetization is, at least in principle, returned to its equilibrium position, as in flip-back methods. However, in the two experiments developed by Kroenke *et al.*[11] the water magnetization evolves differently in the two sequences, which might lead to systematic errors. Moreover, in our hands, we do not see any improvement in the reproducibility of the values of the relaxation rates in terms of standard deviations of identical experiments. This can be attributed to different factors: the phases of the signals are not pure, partly due to homonuclear proton-proton couplings acting in the delays, and partly due to offset effects (titled effective fields) during the pulses. Secondly, the water signal tends to be suppressed less efficiently, leading to small base line distortions. It would be possible to combine the symmetrical reconversion method of

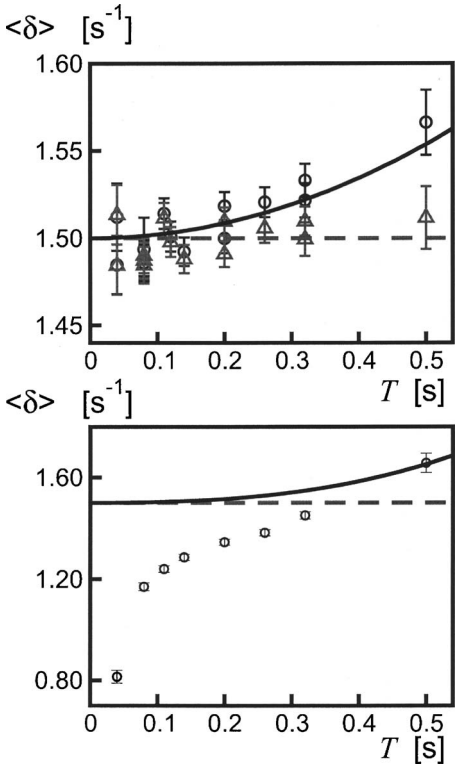

FIG. 3. Results of the experiment of Fig. 2 applied to a sample of ^{15}N labeled human ubiquitin. (Top): Rates $\langle\delta\rangle$ averaged over residues 2-71 are plotted as a function of the relaxation delay T. The open circles were obtained by inserting the peak intensities of the four experiments into Eq. (7) assuming $\Delta=0$. The triangles correspond to the rates $\langle\delta\rangle$ corrected for the difference Δ between the relaxation rates of the operators N_z and $2N_yH_z$ using Eqs. (7) and (8). The dashed line represents the weighted average of the rates represented by the triangles, while the bold line is the theoretical curve obtained from Eq. (7) when combining this average with $\langle\Delta\rangle$. On the bottom are the results obtained with the sequence of Kroenke *et al.*[11] The dashed line lies at the same height as below, while the bold line represents the theoretical curve.

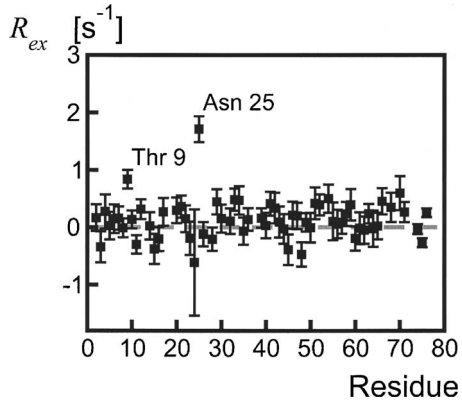

FIG. 4. Amide nitrogen exchange rates R_{ex}(N) obtained from measurements of R_L(N/NH), R_T(N/NH), R_1(N), R_2(N) and σ(H→N) using Eq. (37), for all residues in ^{15}N labeled human ubiquitin.

Fig. 1(b) with the double swapping scheme of Fig. 1(c). However, calculations indicate that such a combination would not improve the accuracy.

The circles in Fig. 3 (top) indicate values δ averaged over residues 2–70 obtained using Eq. (1) for different relaxation delays T. Since the protein was not deuterated, a significant difference between the autorelaxation rates of N_z and $2N_zH_z^N$ operators is observed. The triangles in Fig. 3 (top) correspond to rates that have been corrected using Eq. (7), inserting Δ obtained from an exponential fit of the ratios of the signal amplitudes A_{II} and A_{III} according to Eq. (8). The dashed line corresponds to the weighted average δ of these values, while the bold line corresponds to the theoretical curve of the rates obtained from Eq. (7), using averages of δ and Δ. In Fig. 3 (bottom), the average values of δ obtained with the sequence of Kroenke *et al.*[11] are plotted as a function of the relaxation time T. One can see that the deviations are particularly large for short times. The deviations are most likely due to remaining diagonal elements in the matrix of Eq. (29), which can arise from incorrect ^{15}N pulse calibration and B_1 inhomogeneity. These artifacts could in principle be diminished by phase alternating the phase of the first ^{15}N pulse of the two swapping blocks, as has been done in the new sequence of Fig. 2. However, this would neither remove artifacts due to the nonideal swapping matrix of Eq. (25) nor compensate for errors due to differences in detection efficiencies of the terms $2N_zH_z^N$ and N_z. The dashed lines in Fig. 3 (top) and (bottom) are at the same height (note the different vertical scales), while the bold line in Fig. 3 (bottom) represents the theoretical rate that is obtained if one does not take into account the difference Δ in autorelaxation rates. With the conventional sequence it is not possible to correct for deviations due to the difference in relaxation rates between $2N_zH_z^N$ and N_z, unless this difference can be determined by independent measurements.

Figure 4 shows the exchange rates R_{ex}(N) that have been obtained by combining longitudinal and transverse auto- and cross-correlated relaxation rates,[11]

$$R_{ex}(\mathrm{N}) = R_2(\mathrm{N}) - \{R_1(\mathrm{N}) - 1.25\sigma(\mathrm{H}\rightarrow\mathrm{N})\} \times \frac{R_T(\mathrm{N/NH})}{R_L(\mathrm{N/NH})} - 1.08\sigma(\mathrm{H}\rightarrow\mathrm{N}), \quad (37)$$

where R_L(N/NH) (=δ) and R_T(N/NH) are the longitudinal and transverse CSA/DD cross-correlated relaxation rates, $\sigma(\mathrm{H}\rightarrow\mathrm{N})=(\gamma_N/\gamma_H)(\eta-1)R_1(\mathrm{N})$ and where the Overhauser enhancement η is given by the ratio of the intensities of the ^{15}N signals in experiments with and without proton saturation. Of all the residues for which a value of R_{ex} could be extracted, only two show significant chemical exchange: threonine 9 and asparagine 25. The latter is well known for showing line broadening due to chemical exchange.[28–31] However, the accuracy, precision, or sample conditions of previous studies of ubiquitin have not permitted to observe a small exchange contribution to the transverse ^{15}N relaxation rate of Thr9. On the other hand, relaxation rates of multiple-quantum ^{15}N–H^N coherences at 280 K indicated that the ^{15}N–H^N pair of Thr9 was involved in a chemical exchange process.[31]

The new experiment of Figs. 1(b) and 2 also allows one to measure accurately the temperature dependence of the order parameter S^2. We start by combining the longitudinal and transverse cross-correlation rates,

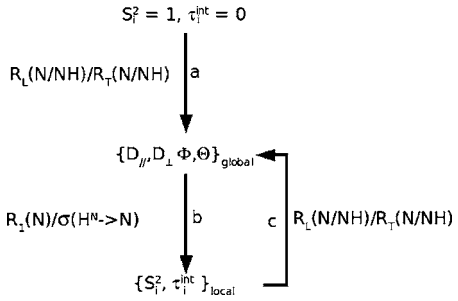

FIG. 5. Flow chart that indicates how the axially symmetric rotational diffusion tensor and parameters of internal motion have been determined. (a) From the ratio $R_L(\mathrm{N/NH})/R_T(\mathrm{N/NH})$, approximate parameters of the diffusion tensor are determined assuming that there are no internal motions. (b) With the help of these values and $R_1(\mathrm{N})$ and $\sigma(\mathrm{H}\rightarrow\mathrm{N})$ measurements, an order parameter S_i^2 and an internal correlation time τ_i^{int} are calculated for each residue. (c) These values are then used to calculate more accurate parameters of the rotational diffusion tensor. Steps (b) an (c) are repeated until the calculations converge. In practice these steps were carried out twice.

$$R_T(\mathrm{N/NH}) - \tfrac{1}{2}R_L(\mathrm{N/NH}) = DJ_{\mathrm{N/NH}}(0). \tag{38}$$

In the case of an axially symmetric rotational diffusion tensor and isotropic local motions, the spectral density $J_{\mathrm{N/NH}}(\omega)$ is[32,33]

$$J_{\mathrm{N/NH}}(\omega) = S^2 \sum_{n=1}^{3} \frac{A_n \tau_n}{1+\omega^2\tau_n^2} + [\{1.5\cos^2(\Theta_{\mathrm{N/NH}}) - 0.5\} - S^2]\frac{\tau}{1+\omega^2\tau^2}, \tag{39}$$

where $\Theta_{\mathrm{N/NH}}$ is the angle between the principal axes of the dipolar and the axially symmetric CSA interactions, $A_1 = (1.5\cos^2\Theta_{\mathrm{N}} - 0.5)(1.5\cos^2\Theta_{\mathrm{NH}} - 0.5)$, $A_2 = 3\sin\Theta_{\mathrm{N}}\cos\Theta_{\mathrm{N}}\sin\Theta_{\mathrm{NH}}\cos\Theta_{\mathrm{NH}}\cos\phi_{\mathrm{N/NH}}$, and $A_3 = 3\sin^2\Theta_{\mathrm{N}}\sin^2\Theta_{\mathrm{NH}}\cos 2\phi_{\mathrm{N/NH}}/4$; Θ_{N} and Θ_{NH} are the polar angles of the CSA and the dipolar interaction in the frame

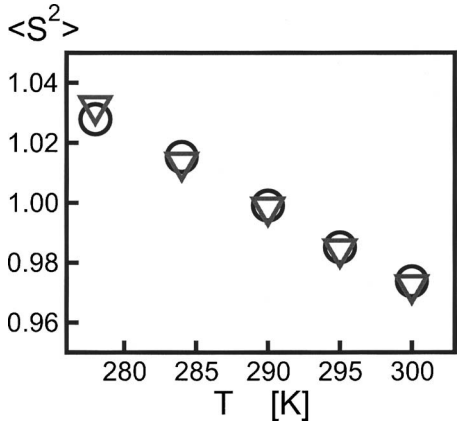

FIG. 6. Temperature dependence of the order parameter $\langle S^2\rangle$ averaged over residues $i=2-70$ as determined by (circles) $R_1(\mathrm{N})$ and $\sigma(\mathrm{H}\rightarrow\mathrm{N})$ measurements (see Fig. 5) and (triangles) $R_L(\mathrm{N/NH})$ and $R_T(\mathrm{N/NH})$ (see text for details). The order parameters S^2 were normalized to give an average of 1 over all temperatures.

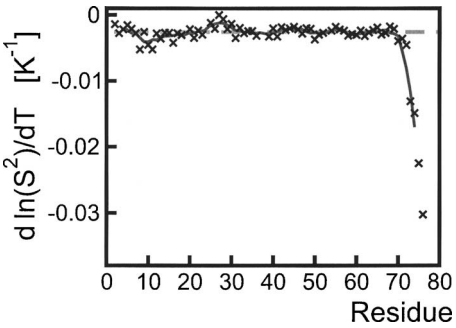

FIG. 7. Derivatives of the logarithm of residue-specific order parameters $\ln(S_i^2)$ with respect to temperature for all residues in ubiquitin. The plot shows the average over the two methods of Fig. 6. The bold line gives the running average over five residues, while the dashed line is the average over all residues except the last four at the C terminus.

of the diffusion tensor; $\phi_{\mathrm{N/NH}}$ is the difference between the azimuthal angles of the CSA and the dipolar interactions; $\tau_1 = 6D_\perp^{-1}$; $\tau_2 = (5D_\perp + D_\parallel)^{-1}$; $\tau_1 = (2D_\perp + 4D_\parallel)^{-1}$; $D_\perp$ is the rotational diffusion coefficient perpendicular to the axis of symmetry of the diffusion tensor; $D_\parallel$ is the rotational diffusion coefficient around this symmetry axis, $\tau^{-1} = \tau^{\mathrm{int}-1} + 4D_\perp + 2D_\parallel$; τ^{int} is the correlation time for the internal motion, and finally, S^2 is the residue-specific order parameter. The parameters of the diffusion tensor can be obtained by fitting the ratios of the longitudinal and transverse cross-correlation rates.[11] The fact that the CSA tensor is not axially symmetric can be taken into account by decomposing the asymmetric CSA tensor into two axially symmetric tensors which can be considered as two independent interactions.[34] We have also corrected for the fact that the second term of Eq. (39) might not be negligible by obtaining the values of the order parameters and the internal correlation times from R_1 and NOE measurements, as indicated in Fig. 5. Since the exact values of the CSA tensor parameters are usually not known, it is not possible to obtain an accurate value of the order parameters. However, we can monitor the changes in order parameters as a function of temperature by dividing DS^2 [where D is the constant of Eq. (38)] by the average $\langle DS^2\rangle$ over all temperatures. In Fig. 6, the average order parameters over all residues (except for the last four C-terminal residues) obtained with this method at five different temperatures are compared with the order parameters obtained from R_1 and NOE measurements. These data show a good agreement between both methods. In Fig. 7, the slope of the variation in order parameter with increasing temperature is plotted as a function of the residue number. Most $\mathrm{NH^N}$ vectors show a comparable temperature dependence of their order parameters. However, flexible regions, like the turn between the first two β strands of ubiquitin (notably residues 8, 10, and 11) as well as the C-terminal tail of the protein (particularly residues 73–76) show a larger increase of their mobility with temperature. This has also been observed in *E. coli* ribonuclease H.[35] On the other hand, the order parameters for the α helix of ubiquitin are high and show a remarkably small dependence on temperature. This indicates that motions of the α helix faster than the overall rotational diffusion of ubiquitin are restricted and contribute

less to the heat capacity of the protein than other secondary structure elements. This is not incompatible with a slow collective motion of the entire α helix[36] on a microsecond time scale.[37]

V. CONCLUSION

We have demonstrated that we can accurately measure longitudinal cross-relaxation rates due to cross-correlated relaxation or Overhauser effects using the principles of symmetrical reconversion combined with swapping of suitable terms in the density operator. Differences between the autorelaxation rates of the different operators involved can be accounted for in a rigorous fashion. We have shown that accurate measurements of longitudinal cross-relaxation rates allow one to obtain reliable estimates of chemical exchange contributions to the decay of transverse ^{15}N magnetization and the temperature dependence of order parameters S^2.

APPENDIX: IDEAL RELAXATION IN THE PRESENCE OF OTHER NUCLEI

When cross-relaxation with other nuclei is averaged, as in Eq. (24), Eq. (1) is exact. To demonstrate this property, we need two conditions: (i) the Liouvillian superoperator that governs relaxation processes must be invariant to the permutation $\hat{S}$ of the two cross-relaxing operators P and Q and (ii) the Liouville subspaces containing the cross-relaxing operators may only be linked by the cross-relaxation process that is to be observed.

Let us consider a Liouvillian superoperator $\hat{L}$ such as $\hat{L}_4^{(0)}$ for which $\hat{S}^{-1}\hat{L}\hat{S}=\hat{L}$, where $\hat{S}$ is the unitary operator that describes the swapping of the operators P and Q, such as $\hat{S}_4^{\mathrm{id}}$. Let us analyze the terms in the denominator of Eq. (1),

$$A_{\mathrm{I}} = P^{+}\exp(-\hat{L}t)P,$$
$$A_{\mathrm{IV}} = Q^{+}\exp(-\hat{L}t)Q. \tag{A1}$$

We have

$$A_{\mathrm{IV}} = P^{+}\hat{S}^{-1}\exp(-\hat{L}t)\hat{S}P = A_{\mathrm{I}}. \tag{A2}$$

Besides the normalization of the signals, Eqs. (18) and (A2) show that symmetrical reconversion and the conventional double swapping approach of Fig. 1(c) generate the same observables under the conditions mentioned above. Let us now separate $\hat{L}$ into two parts,

$$\hat{L} = \hat{L}_a + \hat{L}_c, \tag{A3}$$

where the cross relaxation between operators P and Q is described by

$$\hat{L}_c = \delta\hat{S}. \tag{A4}$$

A straightforward calculation shows that

$$\hat{S}^{-1}\hat{L}_a\hat{S} = \hat{L}_a,$$
$$\hat{L}_a\hat{L}_c = \hat{L}_c\hat{L}_a. \tag{A5}$$

Therefore,

$$\exp(-\hat{L}t) = \exp(-\hat{L}_a t)\exp(-\hat{L}_c t). \tag{A6}$$

Using the closure theorem and the Taylor series of a matrix exponential, one has

$$\exp(-\hat{L}t) = \exp(-\hat{L}_a t)\sum_{Q_i} Q_i Q_i^{+}[\cosh(\delta t)\hat{E} - \sinh(\delta t)\hat{S}], \tag{A7}$$

where $\hat{E}$ is the identity superoperator. In addition, according to condition (ii), $\hat{L}_a$ does not couple the subspaces containing P and Q, so that

$$P^{+}\exp(-\hat{L}_a t)Q = Q^{+}\exp(-\hat{L}_a t)P = 0. \tag{A8}$$

From Eqs. (A1), (A7), and (A8), one can derive

$$A_{\mathrm{I}} = P^{+}\exp(-\hat{L}_a t)P\cosh(\delta t),$$
$$A_{\mathrm{II}} = P^{+}\exp(-\hat{L}_a t)P\sinh(\delta t), \tag{A9}$$
$$\frac{A_{\mathrm{II}}}{A_{\mathrm{I}}} = \tanh(\delta t).$$

The two conditions (i) and (ii) are sufficient to obtain an ideal behavior for the observable, even in the presence of proton-proton cross relaxation.

[1] J. Boyd, U. Hommel, and V. V. Krishnan, Chem. Phys. Lett. **187**, 317 (1991).
[2] B. Reif, M. Hennig, and C. Griesinger, Science **276**, 1230 (1997).
[3] N. Tjandra, A. Szabo, and A. Bax, J. Am. Chem. Soc. **118**, 6986 (1996).
[4] D. Frueh, Prog. NMR Spectrosc. **41**, 305 (2002).
[5] C. Perazzolo, J. Wist, K. Loth, L. Poggi, S. Homans, and G. Bodenhausen, J. Biomol. NMR **33**, 233 (2005).
[6] A. Del Rio, A. Anand, and R. Ghose, J. Magn. Reson. **180**, 1 (2006).
[7] F. Kateb, D. Abergel, Y. Boulquit, P. Duchambon, C. T. Craescu, and G. Bodenhausen, Biochemistry **45**, 15011 (2006).
[8] Y. Pang and E. R. P. Zuiderweg, J. Am. Chem. Soc. **122**, 4841 (2000).
[9] K. Loth, P. Pelupessy, and G. Bodenhausen, J. Am. Chem. Soc. **127**, 6062 (2005).
[10] J. B. Hall and D. Fushman, J. Am. Chem. Soc. **128**, 7855 (2006).
[11] C. D. Kroenke, J. P. Loria, L. K. Lee, M. Rance, and A. G. Palmer III, J. Am. Chem. Soc. **120**, 7905 (1998).
[12] T. Meersmann and G. Bodenhausen, Chem. Phys. Lett. **257**, 374 (1996).
[13] R. Ghose and J. H. Prestegard, J. Magn. Reson. **134**, 308 (1998).
[14] P. Pelupessy, G. M. Espallargas, and G. Bodenhausen, J. Magn. Reson. **161**, 258 (2003).
[15] J. B. Hall and D. Fushman, Magn. Reson. Chem. **41**, 837 (2003).
[16] J. Jeener, Adv. Magn. Reson. **10**, 1 (1982).
[17] F. Ferrage, P. Pelupessy, D. Cowburn, and G. Bodenhausen, J. Am. Chem. Soc. **128**, 11072 (2006).
[18] M. H. Levitt and L. Di Bari, Phys. Rev. Lett. **69**, 3124 (1992).
[19] R. Ghose, Concepts Magn. Reson. **12**, 152 (2000).
[20] C. Zwahlen, S. J. F. Vincent, L. Di Bari, M. H. Levitt, and G. Bodenhausen, J. Am. Chem. Soc. **116**, 362 (1994).
[21] S. J. F. Vincent, C. Zwahlen, P. H. Bolton, T. M. Logan, and G. Bodenhausen, J. Am. Chem. Soc. **118**, 3531 (1996).
[22] J. H. Wu, J. S. Fan, S. M. Pascal, and D. W. Yang, J. Am. Chem. Soc. **126**, 15018 (2004).
[23] C. Eichmüller and N. R. Skrynnikov, J. Biomol. NMR **32**, 281 (2005).
[24] R. Ghose, T. R. Eykyn, and G. Bodenhausen, Mol. Phys. **96**, 1281

(1999).
[25] L. E. Kay, P. Keifer, and T. Saarinen, J. Am. Chem. Soc. **114**, 10663 (1992).
[26] D. J. States, R. A. Haberkorn, and D. J. Ruben, J. Magn. Reson. (1969-1992) **48**, 286 (1982).
[27] M. Piotto, V. Saudek, and V. Sklenar, J. Biomol. NMR **2**, 661 (1992).
[28] D. Fushman, N. Tjandra, and D. Cowburn, J. Am. Chem. Soc. **121**, 8577 (1999).
[29] E. de Alba, J. L. Baber, and N. Tjandra, J. Am. Chem. Soc. **121**, 4282 (1999).
[30] J. L. Mills and T. Szyperski, J. Biomol. NMR **23**, 63 (2002).
[31] F. Massi, M. J. Grey, and A. G. Palmer, Protein Sci. **14**, 735 (2005).
[32] D. E. Woessner, J. Chem. Phys. **37**, 647 (1962).
[33] G. Lipari and A. Szabo, J. Am. Chem. Soc. **104**, 4546 (1982).
[34] M. Goldman, J. Magn. Reson. (1969-1992) **60**, 437 (1984).
[35] A. M. Mandel, M. Akke, and A. G. Palmer, Biochemistry **35**, 16009 (1996).
[36] J. Meiler, W. Peti, and C. Griesinger, J. Am. Chem. Soc. **125**, 8072 (2003).
[37] R. Kitahara, S. Yokoyama, and K. Akasaka, J. Mol. Biol. **347**, 277 (2005).